Vol.2, No.1, 26-31 (2011)
doi:10.4236/jbpc.2011.21004

Journal of Biophysical Chemistry

Features of the formation and nanostructure of the film with the basic hexagonal phase $TiN_{0.3}$ by arc evaporation

Anna L. Kameneva[1], L'ybov N. Guselnikova[2], Tatyana O. Soshina[2]

[1]State educational institution of the higher vocational education Perm state technical university, PSTU, Perm, Russia;
*Corresponding author: annkam789@mail.ru
[2]Branch of PSTU, Lys'va, Russia

Received 27 September 2010; revised 21 October 2010; accept 3 November 2010.

ABSTRACT

Forming and nanostructuring processes of TiN film by electric arc evaporation under the conditions of the reactive nitrogen gas deficit in the gas mixture (30%) have been investigated. The results of a technological experiment, electron microscopic examination, X-ray diffraction phase analysis and mechanical testing of the film revealed that a significant increase in ion density and mobility leads to deterioration of the formation temperature conditions, structural and phase changes in TiN film and change of the main cubic phase (111)TiN on a hexagonal (101)$TiN_{0.3}$. In the end repeated decrease of the the film microhardness with (101)$TiN_{0.3}$ was caused not only by erosion of the film, but also because of change in the processes of its formation and nanostructuring in comparison with similar processes of the film with (111)TiN.

Keywords: TiN Film; Arc Spraying; Forming and Nanostructuring Processes; Structure and Phase Modification

1. INTRODUCTION

It is known [1-27] that films' exploitation conditions depend on raw materials, methods and technological parameters of the application, providing the necessary energy mass transfer of precipitable atoms, ions, molecules, nano and ionized particles. The main technological parameters are: the pressure of the gas mixture, the bias voltage on the substrate, the contents of the reaction gas in the gas mixture, the cathode-substrate distance, arc current (for electric arc evaporation), the temperature of the substrate and film, the maximum rate of deposition.

The aim of this paper is to study the effect of the nitrogen minimum concentration in the gas mixture at the temperature conditions, the direction of preferential crystallographic orientation, phase composition, mechanical conditions, formation and nanostructuring of TiN film during electric-arc evaporation.

2. METHODS OF THE SUBSTRATES PREPARATION, FORMING AND INVESTIGATION OF STRUCTURE AND CONDITIONS OF TiN FILM

2.1. Methods of the Preparation of Substrates and Formation of TiN Film

TiN film was formed on an industrial installation NNV-6.6-I4 with a single arc evaporation with a titanium cathode (s BT1-00) with 30% nitrogen content in the gas mixture. To increase the adhesive strength of TiN film on the surface of the test samples from Article 2 [2], Ti underlayer was applied after its ion cleaning- heating.

2.2. The Method of Substrate and TiN Film Temperature Control

Temperature of test pieces surface as well as the film temperature after each 10 minutes of the film deposition have been measured by infrared contactless pyrometer after both ionic cleaning and sublayer applying, a whole duration of the precipitation process was 30 minutes.

2.3. Methods of Studying the Structure, Phase Composition and Conditions of TiN Film

Morphological traits of the formed films have been investigated by bitmapped electron microscope BS 300 with prefix for microanalysis EDAX Genesis 2000. X-ray diffraction phase analysis of TiN film was carried out using X-ray diffractometer DRON-4 in Cu Kα radiation. Microhardness of the composition has been measured by microhardness tester PMT-3 with indenter load

Copyright © 2011 SciRes.

of 0.5 N after the film precipitation process.

3. SIMULATION RESULTS AND DISCUSSION

Technological parameters of processes for preparing the substrate surface before precipitation process of the film: ion cleaning- heating and deposition of Ti underlayer are shown in **Table 1**, the technological parameters of electric arc evaporation process and microhardness of the composition: the TiN film - substrate (hereinafter the microhardness of the composition) are listed in **Table 2**.

The results of X-ray diffraction phase analysis of TiN film plots, formed by arc evaporation at a nitrogen content in the gas mixture of 30% do not correspond with the previous similar studies of TiN film, formed at different contents of bias potential on the substrate (**Figure 1**, **Tables 3**,**4**). It was found previously [2] that regardless of the bias voltage at a maximum temperature of the film > 700 K and the rate of heating on the substrate > 14.2 K/min, the film is formed, consisting of the main cubic phase of TiN with the direction of preferred crystallographic orientation (111) and more - hexagonal phase $TiN_{0.3}$.

It was established for the first time that the nitrogen content decrease in the gas mixture to 30%, a significant increase in ion density and its mobility, as well as deterioration of the formation temperature conditions (the original film temperature was 613 K, the rate of its heating - 12.0 K/min) lead to a change in the basic cubic phase 111(TiN) to the hexagonal (101)$TiN_{0.3}$ phase, the emergence of new additional phases with volume fractions: tetragonal Ti_2N - 3.7% and hexagonal Ti - 2.1% and more than twofold decrease of the composition microhardness. It ought to be noted that minimal deviation of the interplanar distance from the table value, a maximum width of the peaks of the hexagonal phase (101)$TiN_{0.3}$ and homogeneous internal stresses in the film happened due to unidirectional displacement of the peaks (111)Ti_2N and (101)$TiN_{0.3}$, (111)Ti.

To determine the cause of changes in the mechanical conditions of TiN film, based on the structural characteristics and phase composition, which differs from all previously received TiN film, the morphological features of its surface were studied.

Through a small increase it was possible to find out only the rough surface of TiN film (**Figure 2**).

Based on the results of electron microscopic studies of the film surface at higher magnification it was revealed that the formation and nanostructure processes of the film with the basic hexagonal $TiN_{0.3}$, or cubic TiN phase are different. In constructed thermal conditions two processes consistently occur: the formation of coarse-grained film and when the temperature of the film gets close to 700 K (650 K) - nanostructuring polycrystalline part of the film.

When the initial temperature conditions of formation is 613 K and heating rate is 12.0 K/min coarse-grain film of laminose structure is formed (**Figure 3**). Erosion of the film surface and its maximum surface roughness, as a result of intense bombardment and sputtering lead to

Table 1. Process conditions of ion cleaning- heating and deposition of Ti underlayer.

Process	U, V	Substrate - plazma source distance, mm	T, min	P, Pa	Ifocusing coil, A	Istabilizing coil, A	Iarc, A	V, rpm	Gas	Final temperature, K
Ionic cleaning	high 600	270	5	0.01	1.50	2.50	80	2.5	Ar	651
Sublayer applying	bias 200	270	3	1.0	1.50	2.50	80	2.5	Ar	613

Table 2. Process conditions of the TiN film applying.

N2, %	L, mm	P, Pa	Iarc, A	Ubias, V	Tfilm, K			Vfilm heat, K/min	Hμ, GPa
					tprocess = 10 min	tprocess = 20 min	tprocess = 30 min		
30	270	1.0	80	200	625	635	660	12.0	10.0

Table 3. Structural characteristics of the TiN-based films produced by arc spraying. V is phase inclusion volume fraction, dTi_2N/dTi_2N_{table} is cleavage spacing, $I_{Ti2N}/I_{TiN0,3}$ is intensity ratio of all reflexes of tetragonal Ti_2N phase and hexagonal $TiN_{0,3}$ the one, $maxI_{111Ti2N}/I_{\Sigma}$ and $maxI_{101TiN0.3}/I_{\Sigma}$ are ratios of maximum reflex intensities (111) or (101) to total intensity of all TiN phase reflexes, and β_0 is breadth of X-ray diffraction line.

V, % Ti	V, % Ti_2N	V, % $TiN_{0,3}$	dTi/dTi_{table}, nm	dTi_2N/dTi_2N_{table}, nm	$dTiN_{0,3}/dTiN_{0,3table}$, nm	$I_{Ti}/I_{TiN0,3}$	$I_{Ti2N}/I_{TiN0,3}$	I_{Σ}	$maxI_{002Ti}/I_{\Sigma}$	$maxI_{111Ti2N}/I_{\Sigma}$	$maxI_{101TiN0,3}/I_{\Sigma}$	$maxI_{Ti}/maxI_{TiN0,3}$	$\beta^0_{111}/\beta^0_{101}$
2.1	3.7	94.2	0.2353 / 0.2340	0.2298 / 0.2292	0.2271 / 0.2268	0.03	0.08	119.5	0.03	0.07	0.90	0.07	0.67 / 1.41

Copyright © 2010 SciRes.

Table 4. Positions of the diffraction peaks.

Film	Phase	Lattice type	Grain orientation	$2\theta_{табл}$, grad	2θ, grad
	Ti	Hexagonal	<002>	38,3911	38,25
TiN	Ti_2N	Tetragonal	<111>	39,3267	39,20
	$TiN_{0,3}$	Hexagonal	<101>	39,7086	39,649

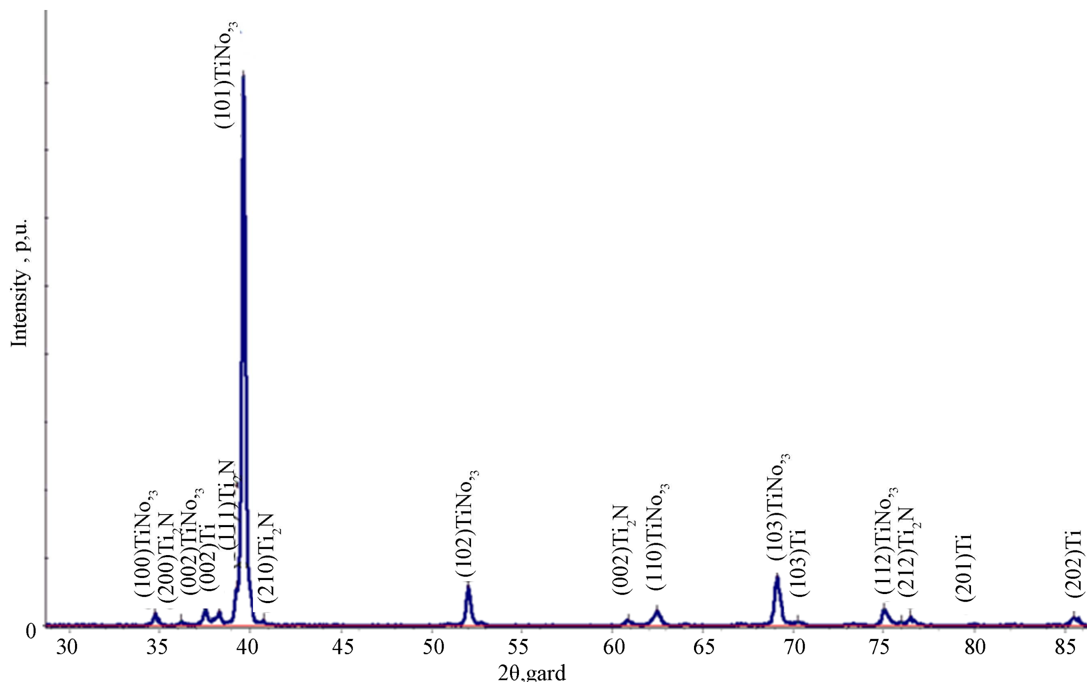

Figure 1. Comparative band of diffractogram fragments for TiN-based film pieces produced by arc spraying with 30% nitrogen content in the gas mixture.

defects in the form of discontinuity at the interface of grains (**Figure 4(a)**), cracking (**Figure 4(b)**), grain pitting (**Figure 4(c)**), and grain boundary fracture of the film **Figure 4(d)**).

It was discovered for the first time that film temperature increase up to 650 K leads to change of processe from coarse-grain film formation to nanostructuring of the polycrystalline film constituent, connected with the following indispensable stage consequence.

- Forming of the globules (**Figure 5(a)**).
- Integration of the globules (**Figure 5(b)**) followed by surface texturing at the end (**Figure 5(c)**).
- Forming of 3D- formations with grain substructure (**Figure 5(d)**).
- Surface coarsening of the 3D- formations with grain substructure (**Figure 5(e)**).
- Nucleation of polycrystalline constituent of the film (**Figure 5(f)**).
- Nanostructuring of the film polycrystalline constituent (**Figure 5(g)**) followed by seed integration to microsystems with incoherent boundaries (**Figure 5(h)**).
- Forming of cone textures <111> on the surface of the 3D-formations with laminose structure (**Figure 5(i)**).

The whole process of nanostructuring polycrystalline constituent of the film is shown in **Figure 6**.

5. CONCLUSION

Phase-structural state of TiN film, formed by electric arc evaporation with a minimum content of nitrogen in the gas mixture (30%) was investigated by X-ray dif-

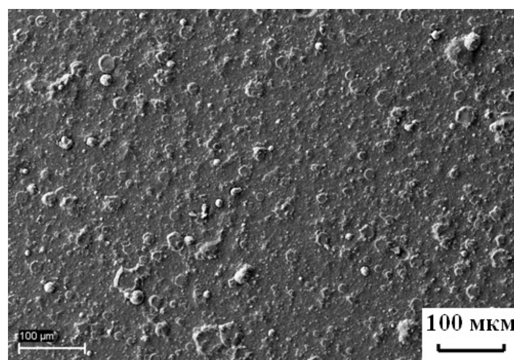

Figure 2. Photomicrographs of TiN films formed by arc spraying at 30% nitrogen concentration in mixed gas.

Copyright © 2011 SciRes.

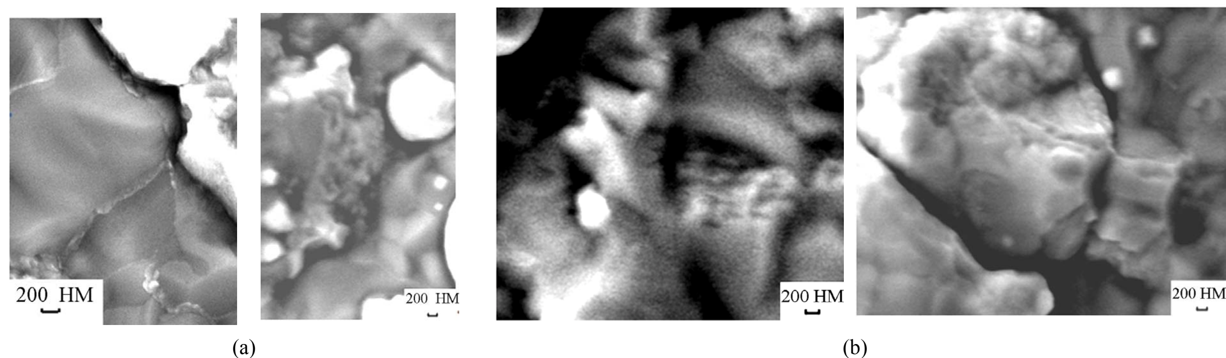

Figure 3. Photomicrograhs of continuous coarse-grained film (a) having laminar grains (b).

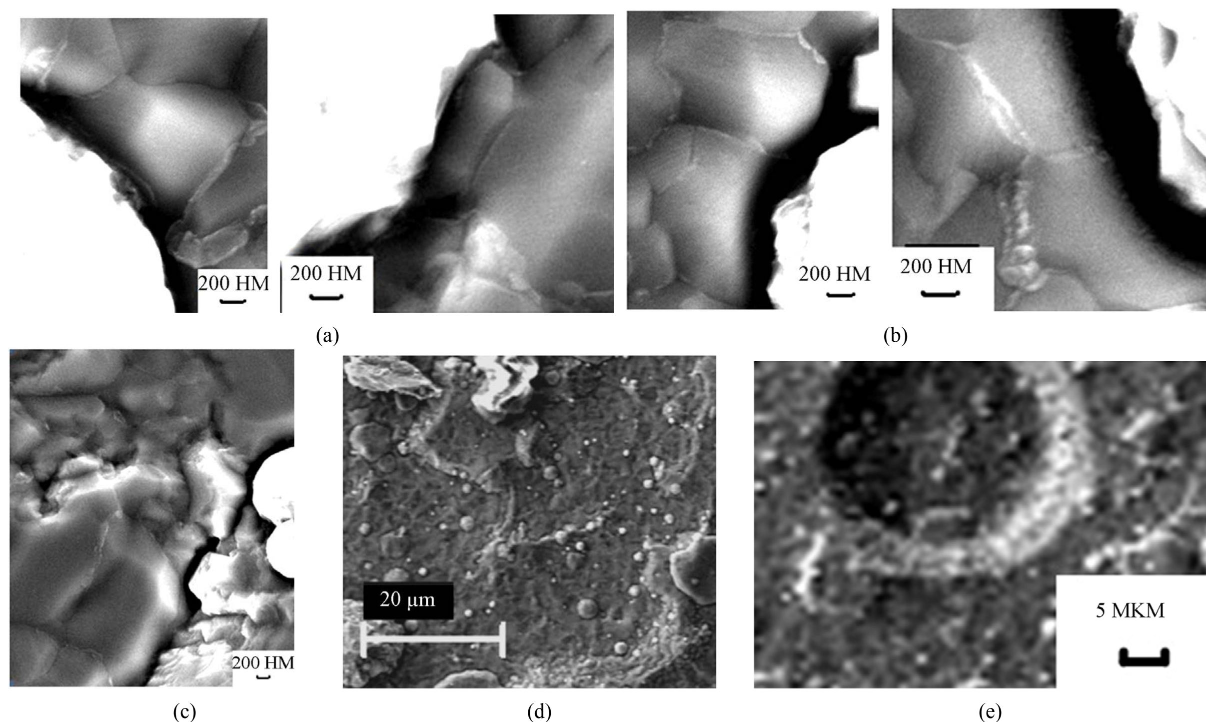

Figure 4. Photomicrographs of TiN film formed at minimum nitrogen concentration (30%) in mixed gas. The film has surface defects: (a) Discontinuity on grain interface; grain (b) Cracking and (c) Roughening; (d) Grain-boundary film destruction, max grain dimensions are 4.5 × 29.0 µm; (e) Discontinuity ("lack") of the film material.

fraction phase analysis method. For the first time ever was established that the maximum possible content of argon in the gas mixture leads to a change in the main phase of the film from a cubic (111)TiN to the hexagonal (101)$TiN_{0.3}$.

Results of electron-microscopic studies of the films surface morphology revealed that at the film temperature less than 650 K coarse-grained film with various defects is formed on the substrate surface. Nanostructuring process of polycrystalline constituent of the film with the main hexagonal $TiN_{0.3}$ phase differs from the same film process with the main cubic (111)TiN phase.

Based on previous experimental studies of the structure and conditions of films formed by nitrogen content in the gas mixture of 90% and a variable bias to the substrate 80 ... 250 V was found that the nucleation of a polycrystalline film with the main component of the cubic phase (111)TiN occurs only at temperatures of films > 700 K and the rate of heating > 14.2 K/min [2].

The obtained results allow to suggest that the main reason for changing the phase ratio in the film, the original course of the process of coarse-grained film formation, and then the process of nanostructuring of poly crystalline constituent of the film with the main component of the hexagonal phase (101)$TiN_{0.3}$, under conditions of low nitrogen content and intensity ion bombardment of the surface forming a film by argon is in sufficient temperature conditions, characterized by the temperature

Copyright © 2010 SciRes.

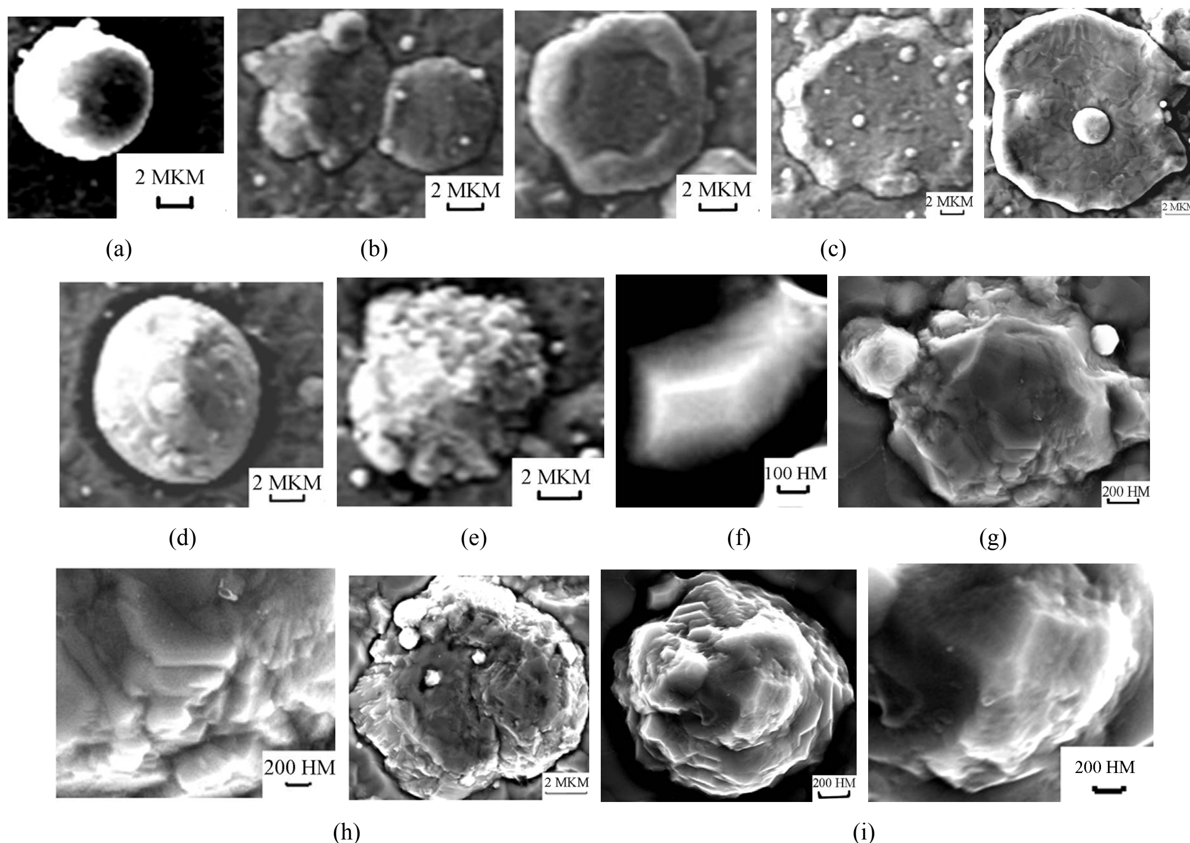

Figure 5. Photomicrograhs of the film having main hexagonal $TiN_{0.3}$ phase on various stages: (a) globular with globule dimension up to Ø9.0 μm; (b) integration of the globules with maximum dimensions of Ø7.5 μm and Ø6.5 μm into structures with length L = 14.0 μm and/or (c) integration of the globules into islands dimensioned up to Ø17.0 μm having globular structure; forming of 3D formations with grain substructure (d) and further their surface coarsening (e) (respectively Ø12.0 μm and Ø9.0 μm); (f) forming of seeds of polycrystalline constituent of the film having form of frustums with upper base dimension of 120x250 μm; (g) forming of laminar 3D formations (Ø4.0 μm) sustaining border coherence, (h) their integration into laminar microsystems (Ø9.0 μm) having non-coherent borders and discontinuity, (i) forming of conic surface structures <111>.

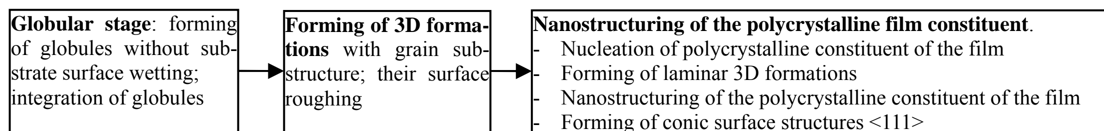

Figure 6. Stages of nanostructuring of TiN films with main hexagonal $TiN_{0.3}$ phase by arc spraying method (~ 660 K, 30% N_2,$V_{film\ heating}$ = 12.0 K / min).

of the film and its rate of heating, nucleation,formation and nanostructure of the film with the main cubic phase (111)TiN.

We can assume that one of the main reasons for double reduction in the microhardness composition is different structural states of formed continuous film-grain lamellar structure and formed on its surface as a result of nanostructuring 3D structures with a lamellar substructure.

REFERENCES

[1] Zhang, Y.J., Yan, P.X., Wu, Z.G., Zhang, W.W., Zhang, G.A., Liu, W.M. and Xue, Q.J. (2005) Effects of substrate bias and argon flux on the structure of titanium nitride films deposited by filtered cathodic arc plasma. *Physica status solidi* (*a*), **202(1)**, 95-101. doi:10.1002/pssa.200406902

[2] Kameneva, A.L., Soshina, T.O. and Guselnikova, L.N. (2010) Effects of substrate voltage bias on forming stages of polycrystalline titanium nitride films by arc spraying. *Materials of XIII International conference High Technology in Russian Industry*, 392-401.

[3] Belyanin, A.F. and Samoylovich, (2004) M.I. Nanostructures and photon crystals. CRTI, Moscow.

[4] Mayrhofer, P.H., Kunc, F., Musil J. and Mitterer, C. (2002) A comparative study on reactive and non-reactive

Copyright © 2011 SciRes.

unbalanced magnetron sputter deposition of TiN coatings. *Thin Solid Films*, **415(9)**, 151-159.
doi:10.1016/S0040-6090(02)00511-4

[5] Musil, J. (2000) Hard and superhard nanocomposite coatings. *Surface and Coatings Technology*, **125(1-3)**, 322-330.
doi:10.1016/S0257-8972(99)00586-1

[6] Veprek, S. (1999) The search for novel superhard materials. *Journal Vacuum Science Technology*, *A*, **17(5)**, 2401-2020.
doi:10.1116/1.581977

[7] Voevodin, A.A., Zabinski, J.S. (2000) Supertough wear-resistant coatings with 'chameleon' surface adaptation. *Thin Solid Films*, **370(1-2)**, 223-231.
doi:10.1016/S0040-6090(00)00917-2

[8] Petrov, I., Varna, P.B., Hultman, L., Greene, J.E. (2003) Microstructural evolution during film growth. *Journal Vacuum Science Technology*, *A*, **21(5)**, 117-128.
doi:10.1116/1.1601610

[9] Thornton, J. (1977) High-rate thick-film growth. *Annual Review of Materials Research*, **7**, 239-260.
10.1146/annurev.ms.07.080177.001323

[10] Messier, R., Giri, A.P. and Roy, R.A. (1984) Revised structure zone model for thin film physical structure. *Journal Vacuum Science Technology*, *A*, **2**, 500-503.
doi:10.1116/1.572604

[11] Thornton, J. A. (1986) The microstructure of sputter-deposited coatings. *Journal Vacuum Science Technology*, *A*, **4(6)**, 3059-3056.
doi:10.1116/1.573628

[12] Barna, P.B. and Adamik, M. (1998) Fundamental structure forming phenomena of policrystalline films and the structure zone models. *Thin Solid Films*, **317**, 27-33.
doi:10.1016/S0040-6090(97)00503-8

[13] Kadlec, S., Musil, J. and Vyskoĉil, J. (1992) Growth and properties of hard coating prepared by physical vapor deposition methods. *Surface and Coatings Technology*, **54-55**, 287-296.
doi:10.1016/S0257-8972(09)90064-0

[14] Hultman, L. (2000) Thermal stability of nitride thin films. *Vacuum*, **57(1)**, 1-30.
doi:10.1016/S0042-207X(00)00143-3

[15] Bunshah, R.F. (1994) Handbook of Deposition technologies for films and coatings: Science, technology and applications. 2nd Edition, Noyes Publications, Park Ridge.

[16] Maissel, L.I. (1983) Handbook of thin films. McGraw-Hill, New York

[17] Messier, R. (1986). Toward quantification of thin film morphology. *Journal of Vacuum Science & Technology A*: *Vacuum*, *Surfaces*, *and Films*, **4(3)**, 490-495.
doi:10.1116/1.573866

[18] Louro, C., Cavaleiro, A., Dub, S., Smid, P., Musil, J. and Vlcek, J. (2002) The depth profile analysis of W-Si-N coatings after thermal annealing. *Surface and Coatings Technology*, **161(2-3)**, 111-119.
doi:10.1016/S0257-8972(02)00325-0

[19] Stüber, M., Leiste, H., Ulrich, S., Holleck, H. and Schild, D. (2002) Microstructure and properties of low friction TiC-C nanocomposite coatings deposited by magnetron sputtering. *Surface and Coatings Technology*, **150(2-3)**, 218-226.
doi:10.1016/S0257-8972(01)01493-1

[20] Andrievski, R.A. and Kalinnikov, G.V. (2001) Physical-mechanical and physical-chemical properties of thin nanostructured boride/nitride films. *Surface and Coatings Technology*, **142-144**, 573-578.
doi:10.1016/S0257-8972(01)01246-4

[21] Antsiferov V.N. and Kameneva, A.L. (2007) Experimental study of the structure of multicomponent nanostructured coatings on the basis of Ti-Zr-N alloys formed by ionic plasma methods. *Russian Journal of Non-Ferrous Metals*, **48(6)**, 488-495.
doi:10.3103/S1067821207060211

[22] Shtansky D.V., Kaneko K., Ikuhara Y. and Levashov. (2001) Characterization of nanostructured multiphase Ti-Al-B-N thin films with extremely small grain size. *Surface and Coatings Technology*, **148(2-3)**, 206-215.
doi:10.1016/S0257-8972(01)01341-X

[23] Shtansky, D.V., Levashov, E.A., Sheveiko, A.N. and Moore, J.J. (1999) Synthesis and Characterization of Ti-Si-C-N Films. *Metallurgical and Materials Transaction* ***A***, **30(9)**, 2439-2447.
doi:10.1007/s11661-999-0252-0

[24] Gupper, A., Fernandez, A., Fernandez-Ramos, C., Hofer, F., Mitterer, C. and Warbichler, P. (2002) Characterization of nanocomposite coatings in the system Ti-B-N by analytical electron microscopy and X-ray photoelectron spectroscopy. *Chemical Monthly*, **133(6)**, 837-848.
doi:10.1007/s007060200056

[25] Mollart, T.P., Gibson, P.N. and Baker, M.A. (1997) An EXAFS and XRD Study of the Structure of Nanocrystalline Ti-B-N Thin Films. *Journal of Physics D: Applied Physics*, **30(13)**, 1827-1832.
doi:10.1088/0022-3727/30/13/001

[26] Gissler, W. (1994) Structure and properties of Ti-B-N coatings. *Surface and Coatings Technology*, **68/69**, 556-563.
doi:10.1016/0257-8972(94)90217-8

[27] Musil, J., Kunc, F., Zeman, H. and Polakova, H. (2002) Relationships between hardness, Young's modulus and elastic recovery in hard nanocomposite coatings. *Surface and Coatings Technology*, **154(2-3)**, 304-313.
doi:10.1016/S0257-8972(01)01714-5

Copyright © 2010 SciRes.